

# Human Meibum and Tear Film Derived (O-Acyl)-Omega-Hydroxy Fatty Acids as Biomarkers of Tear Film Dynamics in Meibomian Gland Dysfunction and Dry Eye Disease

Safal Khanal,<sup>1</sup> Yuqiang Bai,<sup>1</sup> William Ngo,<sup>2,3</sup> Kelly K. Nichols,<sup>1</sup> Landon Wilson,<sup>4,5</sup> Stephen Barnes,<sup>4,5</sup> and Jason J. Nichols<sup>1</sup>

<sup>1</sup>Department of Optometry and Vision Science, School of Optometry, University of Alabama at Birmingham, Birmingham, Alabama, United States

<sup>2</sup>Centre for Ocular Research & Education, School of Optometry & Vision Science, University of Waterloo, Waterloo, Ontario, Canada

<sup>3</sup>Centre for Eye and Vision Research, 17W Hong Kong Science Park, Hong Kong

<sup>4</sup>Department of Pharmacology and Toxicology, School of Medicine, University of Alabama at Birmingham, Birmingham, Alabama, United States

<sup>5</sup>Targeted Metabolomics and Proteomics Laboratory, University of Alabama at Birmingham, Birmingham, Alabama, United States

Correspondence: Jason J. Nichols, The University of Alabama at Birmingham 1716 University Blvd, Birmingham, AL 35233, USA; [jjn@uab.edu](mailto:jjn@uab.edu).

Received: April 22, 2021

Accepted: June 7, 2021

Published: July 8, 2021

Citation: Khanal S, Bai Y, Ngo W, et al. Human meibum and tear film derived (O-Acyl)-omega-hydroxy fatty acids as biomarkers of tear film dynamics in meibomian gland dysfunction and dry eye disease.

*Invest Ophthalmol Vis Sci.* 2021;62(9):13.

<https://doi.org/10.1167/iovs.62.9.13>

<https://doi.org/10.1167/iovs.62.9.13>

**PURPOSE.** To investigate the association between precorneal tear film (PCTF)- and meibum-derived (O-Acyl)-omega-hydroxy fatty acids (OAHFAs) and PCTF thinning in meibomian gland health and dysfunction.

**METHODS.** Of 195 eligible subjects (18–84 years, 62.6% female), 178 and 170 subjects provided both PCTF optical coherence tomography (OCT) imaging and mass spectrometry data for tears ( $n = 178$ ) and meibum ( $n = 170$ ). The PCTF thinning rate was measured in the right eye using an ultra-high-resolution, custom-built OCT. Tear and meibum samples from the right eye were infused into the SCIEX 5600 TripleTOF mass spectrometer in the negative ion mode. Intensities ( $m/z$ ) of preidentified OAHFAs were measured with Analyst 1.7TF and LipidView 1.3 (SCIEX). Principal component (PC) analyses and Spearman's correlations ( $\rho$ ) were performed to evaluate the association between OAHFAs and PCTF thinning rates.

**RESULTS.** In meibum and tear samples, 76 and 78 unique OAHFAs were detected, respectively. The first PC scores of the meibum-derived OAHFAs had statistically significant correlations with PCTF thinning rates ( $\rho = 0.18$ ,  $P = 0.016$ ). Among 10 OAHFAs with the highest first PC loadings, six OAHFAs had negative correlations with PCTF thinning rate (18:2/16:2,  $\rho = -0.19$ ,  $P = 0.01$ ; 18:2/30:1,  $\rho = -0.21$ ,  $P = 0.008$ ; 18:1/28:1,  $\rho = -0.22$ ,  $P = 0.004$ ; 18:1/30:1,  $\rho = -0.22$ ,  $P = 0.005$ ; 18:1/25:0,  $\rho = 0.22$ ,  $P = 0.006$ ; and 18:1/26:1,  $\rho = -0.22$ ,  $P = 0.006$ ), while one OAHFA had a positive correlation with PCTF thinning rate (18:2/18:1,  $\rho = 0.48$ ,  $P = 0.006$ ). Tear film-derived OAHFAs had no association with the PCTF thinning rate.

**CONCLUSIONS.** Several human meibum-derived OAHFAs showed significant associations with PCTF thinning, suggesting that these OAHFAs could be implicated in the mechanism underlying the stabilization and thinning of the PCTF. The tear-film derived OAHFAs were, however, independent of the rate of PCTF thinning.

**Keywords:** tear film, (O-Acyl)-omega-hydroxy fatty acids, lipids, meibum, precorneal tear film, tear film lipid layer, meibomian gland, dry eye disease

A thin film (~2 to 5  $\mu\text{m}$ )<sup>1–3</sup> of semiviscous tear fluid covers the ocular surface. Shortly after a blink, the human precorneal tear film (PCTF) thins and breaks up abruptly (~seconds), but again spreads over the ocular surface and restores its thickness following redistribution by a subsequent blink.<sup>4</sup> The PCTF thinning is primarily due

to evaporative loss of aqueous from the PCTF rather than other mechanisms, such as tangential or radial fluid flow or gravity.<sup>4–6</sup> When aqueous evaporation is excessive, a cascade of events is initiated, resulting in tear hyperosmolarity and inflammatory damage to the ocular surface.<sup>7–9</sup> According to the Tear Film Ocular Surface Society (TFOS) Dry Eye

Workshop (DEWS II), evaporation-induced tear film instability is a hallmark mechanism that triggers the vicious cycle of dry eye disease (DED).<sup>10,11</sup>

Overlying the mucoaqueous phase of the human tear film is a thin layer of lipids (mean 42 nm, range, 15 to 157 nm)<sup>12</sup> that forms a barrier against evaporative aqueous loss,<sup>9,13–16</sup> and renders elasticity to the air-tear surface, providing resistance to stretching and thinning deformations and conferring mechanical stability to the tear film.<sup>17–19</sup> This tear film lipid layer (TFLL) consists of a complex mixture of non-polar (e.g., wax esters, cholesteryl esters) and polar lipids (e.g., phospholipids, (O-Acyl)-omega-hydroxy fatty acids [OAHFAs]),<sup>19–21</sup> which are predominantly derived from meibum secreted by the meibomian glands.<sup>22,23</sup> Therefore the ability of the TFLL to retard evaporation and protect against aqueous loss depends to a large extent on meibomian gland health. Qualitative or quantitative alterations in meibum resulting from meibomian gland dysfunction (MGD) may affect PCTF structure, function, and dynamics and may produce deficiencies in lipid constituents of the TFLL, inhibiting its ability to spread the nonpolar lipids evenly over the mucoaqueous phase.<sup>10,24</sup> Indeed, MGD is recognized as the leading cause of evaporative DED.<sup>10,25</sup> Studies have shown that the expression of meibum increases PCTF stability and TFLL thickness<sup>26</sup> and decreases the rate of tear evaporation in healthy subjects and those with coexisting DED and MGD.<sup>27</sup> Conversely, the PCTF has been found to be unstable and the rate of tear evaporation increased in subjects with absent or less confluent lipid layer.<sup>14</sup> Clinical and population-based studies also indicate a high rate of comorbidity of MGD and DED,<sup>24,28–32</sup> suggesting a strong association between meibomian gland health and PCTF organizational characteristics.

Although changes in PCTF dynamics are better established in DED, the molecular mechanisms or alterations underlying these physiological changes have yet to be fully understood. This is partly due to the complex relationship between the TFLL thickness and PCTF thinning, because studies have shown at best a modest negative association between these two parameters, with some even reporting a positive association between thicker TFLL and clinical signs of DED.<sup>6,33</sup> These findings have stimulated the hypothesis that the TFLL interacts with other tear film constituents (e.g., mucins, proteins, and salts) to function as an antievasive barrier.<sup>19</sup> However, factors other than TFLL structure (thickness) such as the biochemical composition are becoming recognized as being critical.<sup>34,35</sup> A growing body of literature now suggests that the TFLL composition and the biophysical properties of its constituents may control the rate of PCTF thinning or evaporation of tears from the ocular surface.<sup>21,36–41</sup>

Of all tear film lipids, OAHFAs, a subclass of amphiphilic anionogenic lipids more recently discovered in human meibum,<sup>42</sup> are a strong lipid biomarker candidate involved in maintaining the TFLL<sup>41,43</sup> and imparting a direct evaporation-resistant effect to stabilize the PCTF.<sup>44,45</sup> Several studies have demonstrated the presence of OAHFAs in human meibum and tear film<sup>46–50</sup> and suggested their potential role in PCTF thinning and stabilization.<sup>43,50,51</sup> In mice, deficiency of OAHFA-producing  $\omega$ -hydroxylase Cyp4f39 fatty acid led to dry eyes and MGD.<sup>43</sup> Cyp4f39-deficient mice also showed decreases in specific OAHFAs and their derivatives, suggesting that this reduction likely caused DED and MGD, although findings were somewhat inconclusive because of limited sample size, no changes in other major

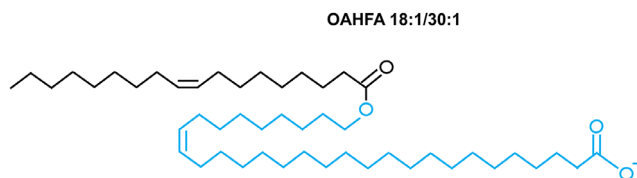


**FIGURE 1.** Schematic diagram of the structure of OAHFA18:1/30:1, which contains 18 carbons in the fatty acid chain (*black*) and 30 carbons in the hydroxyl fatty acid chain (*blue*), with one double bond in each chain.

OAHFAs, and confounding observations such as corneal epithelial damage, which may have instead contributed to the observed dry eye.<sup>43</sup> In humans, OAHFAs were found to decrease with increasing severity of DED<sup>49</sup> and increase after eyelid warming treatment in MGD.<sup>51</sup>

On the basis of these findings, it is hypothesized that OAHFAs are implicated in the mechanism underlying the destabilization and thinning (evaporation) of the PCTF. The present study was designed to test this hypothesis by investigating the association between the abundance of meibum- and tear film-derived OAHFAs with PCTF structural characteristics.

## MATERIALS AND METHODS

Ethics approval for this study was obtained from the Institutional Review Board of the University of Alabama at Birmingham. Each subject gave informed consent in writing before participation in the study, and all study procedures adhered to the tenets of the Declaration of Helsinki.

### Nomenclature

OAHFAs are large molecular weight molecules of a fatty acid esterified with an omega-hydroxy fatty acid. The number of bonds in the aliphatic chain determines their degree of saturation. Saturated OAHFAs contain no double bonds, whereas unsaturated OAHFAs contain one or more double bonds.<sup>52</sup> Standard nomenclature for OAHFAs is used in this study,<sup>53,54</sup>; OAHFA X1:Y1/X2:Y2, where X1 and Y1 denote the number of carbons and double bonds in the fatty acid component, respectively, and X2 and Y2 denote the number of carbons and double bonds in the omega-hydroxy fatty acid component, respectively. **Figure 1** shows the structure of an example OAHFA 18:1/30:1.

### Human Subject Recruitment

To determine the eligibility of subjects for participation in the study, a prescreening was carried out among subjects who had previously provided consent to be contacted for future studies as part of the University of Alabama at Birmingham Clinical Eye Research Facility IRB approved recruitment databases and procedures. Subjects were included if they were non-contact lens wearers and 18 years of age or older. Subjects receiving eye care for acute ocular diseases (except MGD or DED), currently using topical ophthalmic lubricants or medications, having health or ocular conditions that could impact meibomian gland function or tear film parameters, and currently participating in any other

intervention-based clinical research study, were excluded. Based on the prescreening, a total of 222 subjects consented to participate in the study.

### Clinical Protocol

All subjects attended a single study visit in the Clinical Eye Research Facility at the University of Alabama at Birmingham. After a detailed ocular and systemic history, subjects completed the Ocular Surface Disease Index (OSDI) questionnaire<sup>55</sup> and underwent a comprehensive examination of the adnexa and ocular surface including tear film imaging.<sup>56</sup> The expressibility and quality of meibum from the meibomian gland orifices were examined by applying firm digital pressure to the lower eyelid. Each gland was graded on a scale of 0 to 3, with 0 representing clear fluid, 1 representing cloudy liquid, 2 representing cloudy with debris, and 3 representing toothpaste-like thick secretion.<sup>57</sup> The sum of the grades from the central eight glands provided the clinical meibum grade score. Based on the OSDI and meibum grade score, each subject was classified into one of the four disease classification groups, adapted from the TFOS International Workshop on MGD guidelines: Normal (OSDI < 13 and meibum grade < 10), MGD (OSDI ≥ 13 and meibum grade ≥ 10), Asymptomatic MGD (OSDI < 13 and meibum grade ≥ 10), and Mixed (OSDI ≥ 13 and meibum grade < 10).<sup>58</sup>

Tear film imaging techniques are described elsewhere.<sup>56</sup> Briefly, cross-sectional OCT images of the tear film were captured from the right eye of each subject in a dimly illuminated room at a controlled temperature (23°–25°C) and humidity (30%–50%). During imaging, subjects were instructed to blink three times and then keep their eyes wide open and steady for as long as possible. To avoid transients because of vertical drift of the tear film after blinks, the image capture was initiated approximately 2.5 seconds after the third blink. Each subject had their right eye imaged twice to obtain two sets of images/videos. After tear film imaging, tears and meibum samples were collected from the right eye of each subject using collection methods optimized for collecting tear film and meibum OAHFAs, as described previously.<sup>48,59–63</sup>

### OCT Imaging

A combined ultra-high-resolution OCT and thickness-dependent fringes interferometer system was used to image the tear film in vivo. This system is capable of capturing images of the tear film with an axial resolution of 1.38 μm. A detailed description of the optical design of this system is available elsewhere.<sup>64</sup> In brief, the OCT system houses a broadband superluminescent diode (T850-HP; Superlum Diodes, Ltd, Moscow, Russia) with a central wavelength of 840 nm and a full-width half-maximum of 175 nm as an illumination source, whereas the thickness-dependent fringe system consists of a Quartz Tungsten-Halogen Lamp (QTH10; Thorlabs, Newton, NJ, USA). During imaging, the OCT system captures eight horizontal line scans (each comprising of 128 A-lines), evenly spaced along a superior-inferior axis, within a 3 mm-diameter central zone. The acquisition time of each OCT C-scan is approximately 30 ms at a rate of 32 frames per second.

### Mass Spectrometry

A semitargeted direct infusion electrospray MS and MS/MS<sup>ALL</sup> in the negative ion mode was performed on a TripleTOF 5600 mass spectrometer (SCIEX, Framingham, MA, USA) to assess the abundance of OAHFAs in tear and meibum samples. This analytical approach has been previously validated to provide reliable assessments of lipids in small volumes of the tear film and quantify concentrations of polar lipids, including OAHFAs.<sup>48,61</sup> The extraction and mass spectrometry analysis protocols associated with this technique have been described in detail in prior reports.<sup>61,63</sup>

### Data Analyses

The rates of PCTF thinning were calculated using linear regression fits of PCTF thicknesses derived from the temporal series of OCT images, as described previously.<sup>56,64</sup> Data on PCTF thinning rates for each disease classification group are available elsewhere.<sup>56</sup> For the analysis of MS data, peak intensities of individual OAHFAs identified in meibum and tear samples were normalized by the internal standard intensity to obtain standard-corrected intensity. Data were then imported and analyzed in R<sup>65</sup> and RStudio.<sup>66</sup> To avoid issues in downstream analyses, intensities of undetected OAHFAs (zero values) were replaced with a small imputed value (one-fifth of the minimum peak intensity of a particular OAHA). Data corrected by internal standard were then normalized by the total ion current, mean-centered and subjected to Pareto scaling. For dimensionality reduction, principal component (PC) analyses were performed using “prcomp” function of the “stats” package (v3.6.2) to project the high-dimensional data to a few components that capture most of the variation in the data. Data on tears and meibum OAHFAs were analyzed separately.

The primary outcome of this study was the association between the abundance of OAHFAs and PCTF thinning rate (evaporation). Because some PC scores (weighted average of all features) and PCTF thinning measures were not normally distributed, the associations between PCs (first and second) and PCTF thinning rates were analyzed using Spearman's correlations ( $\rho$ ). If the association was significant, the absolute loadings of the PCs were ranked, and a list of 10 OAHFAs that had the highest loadings and contributed the most to the PC was derived. Finally, Spearman's correlations were performed to evaluate the association between standard-corrected intensity of these OAHFAs and PCTF thinning rate. Data are expressed as mean ± standard deviation of the mean unless otherwise stated. The value of alpha was set at 0.05 for statistical significance.

## RESULTS

### Baseline Characteristics

Of the 222 subjects consented, 195 were eligible based on classifications conducted using data collected during the clinical examination. Out of these 195 subjects (age 18–84 years; 62.6% female), 178 subjects had both tear film samples and imaging data collected, while 170 subjects had both meibum samples and imaging data collected. The Table summarizes the baseline characteristics of these subjects.

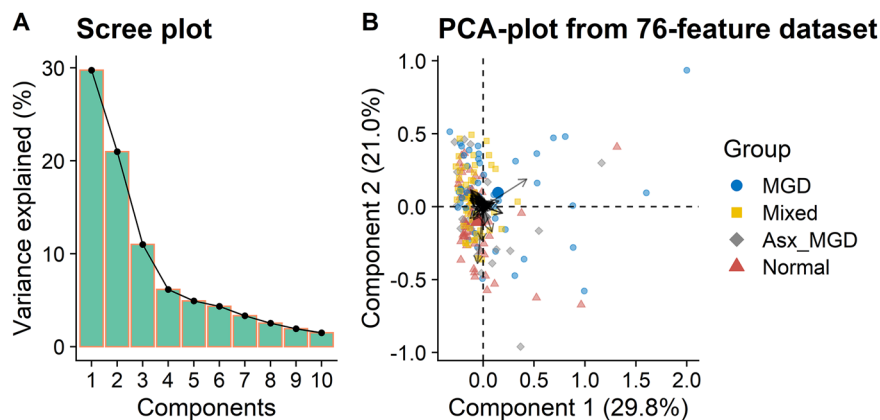


**FIGURE 2.** PC analysis of meibum-derived OAHFAs. (A) Scree plot showing the proportion of variance explained by the first 10 PCs. (B) PC biplot showing sample scores stratified by the four disease classification groups and feature loadings (black arrows).

**TABLE.** Baseline Characteristics of the Study Subjects

	Tears	Meibum
Number of subjects	178	170
Total OAHFAs	78	76
Gender		
Male	65	66
Female	113	104
Age (y), mean (SD)	39.3 (14.2)	39.4 (14.3)
Ethnicity		
Hispanic	1	1
Non-Hispanic	177	169
Race		
Asian	18	19
African American	93	88
Caucasian	65	60
Other	2	3
Volume collected (μL), mean (SD)	0.03 (0.01)	0.03 (0.01)

**Meibum-Derived OAHFAs**

A total of 76 unique OAHFA species were identified in meibum across all subject samples. Figure 2 shows the results of the unsupervised multivariate analyses conducted using the PC method that included all 76 features. As shown in the scree plot (eigenvalues or proportion of variances of PCs) in Figure 2A, the first two PCs captured more than 50% of the variation in the data, with the first PC accounting for 29.8% variance, and the second PC accounting for 21.0% variance. Although most samples projected into a small region forming a narrow herd as illustrated by the PC scores in Figure 2B, a few samples were separated from the herd, indicating some separation among the four classification groups. However, there was little difference among the contributions of the features (black arrows in Fig. 2B). Among the 76 OAHFAs (features), one OAHFA (18:2/16:2) showed a relatively large vector length, suggesting a significantly greater contribution to the PCs than other OAHFAs (features).

To evaluate the association between the PCs and imaging parameters, Spearman’s correlation analyses were conducted between the sample scores obtained from PC analyses and PCTF thinning rate (Fig. 3). Although the first PC scores correlated positively with PCTF thinning rate ( $\rho = 0.18, P = 0.016$ ), the second PC scores were not associated

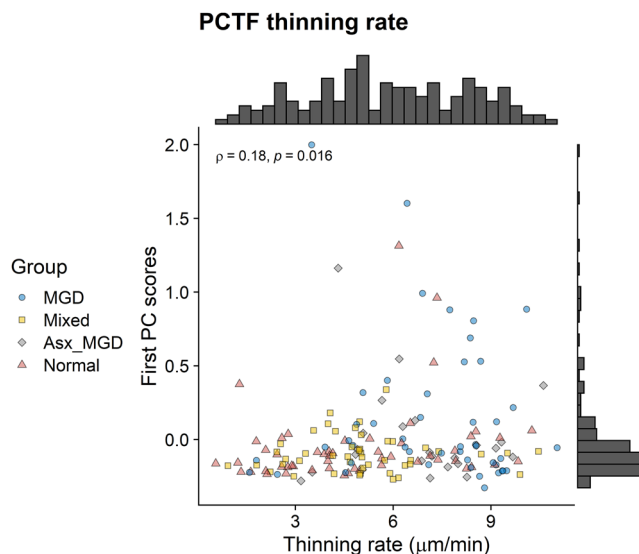


**FIGURE 3.** Distributions of the first PC scores of the meibum-derived OAHFAs as a function of PCTF thinning rate. There was a significant positive correlation between the first PC scores and PCTF thinning rate.

with PCTF thinning rate ( $\rho = -0.01, P = 0.89$ ). In addition, no significant associations were found between the first PC scores and PCTF thickness ( $\rho = 0.10, P = 0.18$ ) or average noninvasive keratography break-up time ( $\rho = -0.09, P = 0.24$ ).

To identify the most contributing OAHFAs, the absolute values of the first PC loadings of all features were ranked in descending order, and 10 OAHFAs with the highest loadings were selected. Figure 4 shows the correlations between the abundance of these OAHFAs (expressed as standard-corrected intensity) and PCTF thinning rate. One OAHFA (18:0/20:0) was detected in only one sample and therefore omitted from subsequent analysis. Of the other nine OAHFAs, only OAHFA 18:2/18:1 had a positive correlation with PCTF thinning rate ( $\rho = 0.48, P = 0.006$ ), whereas the abundance of the other OAHFAs had negative correlations with PCTF thinning rate. These were: OAHFA 18:2/16:2 ( $\rho = -0.19, P = 0.01$ ), OAHFA 18:2/30:1 ( $\rho = -0.21, P = 0.008$ ), 18:1/28:1 ( $\rho = -0.22,$

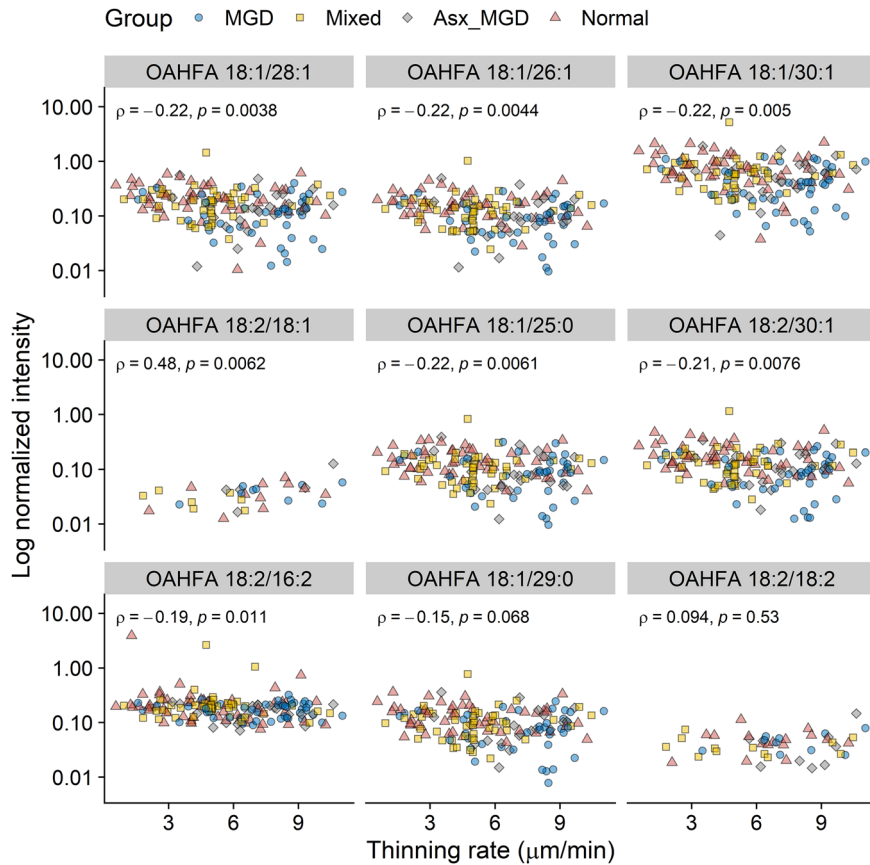


FIGURE 4. Association between PCTF thinning rate and the abundances of OAHFAs that contributed the most to the first PC. Asx\_MGD, asymptomatic MGD.

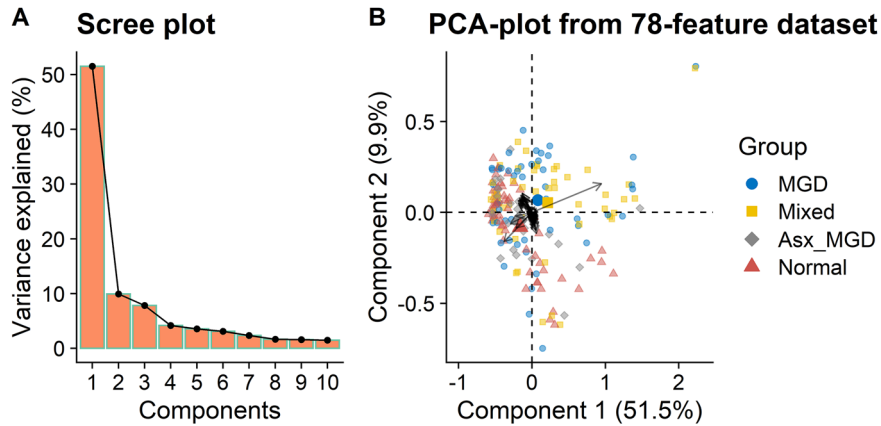


FIGURE 5. PC analysis of PCTF-derived OAHFAs. (A) Scree plot showing the proportion of variance explained by the first 10 PCs. (B) PC biplot showing sample scores stratified by the four disease classification groups and feature loadings (black arrows).

$P = 0.004$ ), 18:1/30:1 ( $\rho = -0.22$ ,  $P = 0.005$ ), 18:1/25:0 ( $\rho = -0.22$ ,  $P = 0.006$ ), and 18:1/26:1 ( $\rho = -0.22$ ,  $P = 0.006$ ). These results indicate that subjects with greater abundances of these OAHFA in their meibum samples had slower rates of PCTF thinning.

**PCTF-Derived OAHFAs**

A total of 78 unique OAHFA species were identified in tear samples across all subjects. Figure 4 illustrates the results

of the PC analyses of these 78 features. As shown in the scree plot (Fig. 5A), the first two PCs explained over 60% of the variation in the data, with the first PC accounting for more than 50% of the variance, and the second PC accounting for approximately 10% variance. The proportion of variance explained by the first two PCs was greater for the tear data (61.4%) than the meibum data (50.8%). Most tear samples projected into a small region forming a narrow herd (Fig. 5B). However, there was a slightly greater separation among the groups when compared with the meibum

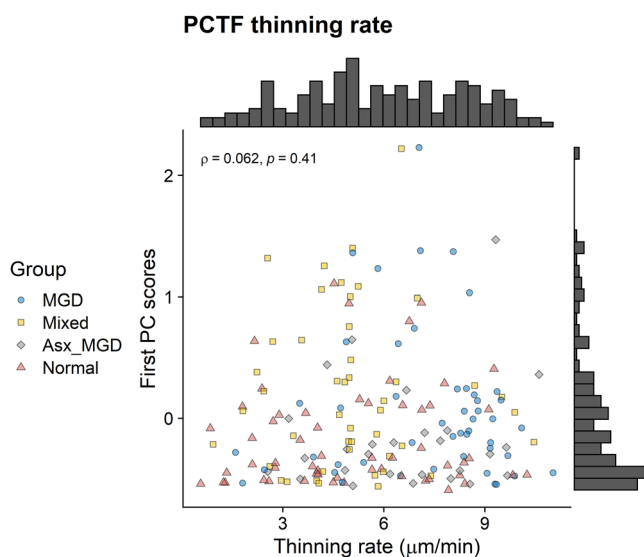


**FIGURE 6.** Distributions of the first PC scores of the PCTF-derived OAHFAs as a function of the PCTF thinning rate. There was no association between the first PC scores and the PCTF thinning rate.

data, and a relatively larger proportion of samples separated from the herd, indicating relatively greater separation among the four disease classification groups. However, the difference among the contributions of the features (black arrows in Fig. 5B) was small. Among the 78 features (OAHFAs), only one feature (OAHFA 18:2/16:2) showed a relatively large vector length (black arrow), suggesting a significantly greater contribution to the PCs than other features.

Spearman's correlation analyses showed no associations between the first PC scores and PCTF thinning rate ( $\rho = 0.06$ ,  $P = 0.41$ , Fig. 6). Similarly, the second PC scores also had no associations with the PCTF thinning rate ( $\rho = 0.03$ ,  $P = 0.66$ ). These results suggested that the PCTF-derived OAHFAs were relatively independent of the thinning rate. In addition, no significant associations were found between the first PC scores and PCTF thickness ( $\rho = -0.06$ ,  $P = 0.42$ ) or average non-invasive keratography break-up time ( $\rho = 0.04$ ,  $P = 0.62$ ).

## DISCUSSION

This study set out to investigate the relationship of the amphiphilic polar lipids, OAHFAs, derived from the human tear film and meibum with PCTF thinning (evaporation). The results of the study showed that the abundance of several meibum-derived OAHFAs varied according to PCTF thinning rate. This finding supports the hypothesis that OAHFAs are implicated in the biochemical mechanism underlying evaporation and PCTF thinning and provide evidence that these polar amphiphilic molecules may serve as a candidate molecular biomarker of the PCTF stability in health and disease.

Consistent with the findings from several previous studies,<sup>46–50</sup> this study also detected a large number of OAHFAs in the human PCTF ( $n = 78$ ) and in meibum ( $n = 76$ ). Several meibum-derived OAHFAs (18:2/18:1, 18:2/16:2, 18:2/30:1, 18:1/28:1, 18:1/30:1, 18:1/25:0, 18:1/26:1) were found to be associated with PCTF thinning, suggesting that these OAHFAs could potentially act as a regulator of PCTF thinning

and stability. What biophysical properties distinguish these OAHFAs from the others and make them particularly relevant to PCTF evaporation remain unknown. Most of these OAHFAs were unsaturated with one or more double bonds in the acyl chain length. Therefore the degree of unsaturation could be a critical property of OAHFAs. The absence of double bonds in saturated fatty acids provides a flexible linear shape allowing for greater association with “self.” By contrast, the presence of one or more double bonds in unsaturated fatty acids makes packing with “self” more difficult. This could allow greater opportunity for interdigitation with the non-polar counterparts (“non-self”), providing better TFL stability and a more effective barrier against PCTF evaporation.<sup>44,67–69</sup> Although most OAHFAs had an inverse association with PCTF thinning rate, suggesting that the abundance of these OAHFAs reduced with an increased rate of PCTF thinning or evaporation, there was a positive relationship between the abundance of OAHFA 18:2/18:1 with PCTF thinning rate. Considering the complex lipid composition of the TFL,<sup>21,70</sup> different OAHFAs may interact differently with the mucoaqueous phase and non-polar lipids and may serve different functions as they relate to tear evaporation.<sup>4,71</sup> It is also possible that the ability of the TFL to retard evaporation depends on a delicate homeostatic balance among several OAHFAs in the TFL.

An important question remains regarding how these specific OAHFAs regulate the rate of PCTF thinning and evaporation. The TFL at the lipid-air interface contains a hydrophobic nonpolar lipid sublayer of cholesterol and wax esters connected to the mucoaqueous phase by the amphiphilic polar lipid sublayer, which predominantly consists of OAHFAs and cholesterol-OAHFAs (~1%–5%), with small amounts of triglycerides, fatty acids, and phospholipids (~1%).<sup>19,23,72</sup> It has been postulated that this polar lipid sublayer, particularly OAHFAs, facilitates retardation of tear evaporation by stabilizing the nonpolar lipid sublayer.<sup>42,72,73</sup> During eye-opening, the upward extension of the mucoaqueous phase (because of negative pressure in the upper eyelid) and the presence of TFL lipids on the lower eyelid region creates a surface pressure gradient, which is nullified by the subsequent upward spreading of TFL on to the mucoaqueous phase.<sup>74</sup> The latter process requires TFL to interact with the mucoaqueous phase and likely involves OAHFAs because of their strong polarity as compared with weakly polar cholesterol and wax esters.<sup>43–45</sup> There is some evidence that the OAHFAs can spread readily over large regions of mucoaqueous phase,<sup>45</sup> retard evaporation and inhibit the development of DED,<sup>41</sup> and exert a direct evaporation-resistant effect, in addition to stabilizing the TFL.<sup>44</sup> Mice deficient in fatty acids involved in OAHFA production ( $\omega$ -hydroxylase Cyp4f39) develop DED and MGD.<sup>43</sup> They also show a reduction of OAHFAs and their derivatives and accumulation of tears on the lower eyelids indicative of increased surface tension.<sup>43</sup> These findings suggest that OAHFAs likely act as surfactants to reduce surface tension at the tears/air interface and thus stabilize TFL to retard tear evaporation and promote PCTF stability.<sup>19,45</sup> It has also been shown that the nonpolar sublayers have no contribution to the evaporation-resisting property of the TFL.<sup>44,75</sup> Furthermore, the defects in the TFL and its coverage across the ocular surface have been reported to primarily drive the rate of tear evaporation.<sup>76</sup> By stabilizing the TFL, OAHFAs presumably reduce structural defects in the lipid layer and guard against evaporation. Whereas the antievaporative function of the TFL may also involve

phospholipids, which have been reported in the polar sublayer of the human lipid layer,<sup>20</sup> the very low concentration of phospholipids in the human tear film (<0.1%<sup>72</sup>) means that they may be unable to interact sufficiently with the nonpolar lipids to stabilize the TFLL.

Compared with the meibum data, the first two PCs explained greater variance in the abundance of tear film-derived OAHFAs, suggesting that the PC technique allowed for significantly better ordination of OAHFAs derived from the PCTF than meibum. It is possible that, unlike meibum, the PCTF contains two distinct sets of OAHFAs: meibomian molecules and oxidized aged molecules. In this regard, the lack of association between tear film-derived OAHFAs and tear film characteristics found in this study is slightly surprising. Tears contain a significantly greater concentration of phospholipids than meibum.<sup>19</sup> These excess phospholipids are likely derived from sources other than meibum (e.g., cells deposited during blinks) and may interact with meibum-derived OAHFAs in their antievaporative functions. Another contributing factor could be the relatively larger variability in the amount of tear film-derived OAHFAs and tear film imaging measures across the subjects (see Fig. 6). Although a high-resolution untargeted MS method as used in this study has been previously shown to provide reliable characterization and quantification of OAHFAs derived from human meibum and tear film,<sup>48,61</sup> this technique yields several candidate lipids requiring a multivariate analytical approach to transform a high-dimensional data to a low-dimensional data. This presents a considerable challenge to investigate the role of specific OAHFAs, particularly if only a few OAHFAs are involved in the mechanism underlying tear evaporation as is evident from the meibum data. Further studies with a targeted approach with a prior chromatographic step may improve our understanding of the role of tear-film-derived OAHFAs in maintaining TFLL and PCTF stability.<sup>47</sup>

In conclusion, this study provides the first evidence of the relationship between OAHFAs and PCTF thinning (evaporation) in a large cohort of healthy and MGD subjects. Results from this study demonstrate that the abundances of several OAHFAs derived from human meibum are associated with PCTF thinning (evaporation); however, OAHFAs derived from the PCTF are independent of the rate of PCTF thinning. The findings of this study are novel and bridge a crucial gap in our understanding of the PCTF homeostasis in health and disease, in addition to providing a basis for further investigations of the mechanistic basis of evaporation-induced PCTF thinning and instability.

### Acknowledgments

The authors thank all individuals involved for their contribution in participant recruitment, data collection, and data management for this study in addition to the participants who provided their time to participate in the clinical visit.

Supported by NIH/NEI R01EY026947 and NIH/NCATs UL1 TR003096. The mass spectrometer was purchased from funding by a NIH Shared Instrumentation Grant S10 RR027822 to SB.

Disclosure: **S. Khanal**, None; **Y. Bai**, None; **W. Ngo**, Centre for Research & Education (CORE) (E), Alcon (R), Allergan (R), Allied Innovations (R), Brien Holden Vision Institute (R), CooperVision (R), GL Chemtec (R), i-Med Pharma (R), Johnson & Johnson

Vision (R), Lubris (R), Menicon (R), Nature's Way (R), Novartis (R), Oté Pharma (R), PS Therapy (R), Safilens (R), Santen (R), Shire (R), SightGlass (R), Visioneering (R); **K.K. Nichols**, Bruder (C, R), Dompe (C, R), Kala (C, R), Novartis/Shire (Medical Exchange International) (C, R), Osmotica, Oyster Point (C, R), Sight Sciences (C, R), Tear Film Innovations/Alcon/Acquiom (C, R), Thea (C, R), Tarsus (C, R), TopiVert (C, R), Allergan (R), Kala (R), Tear Science (R); **L. Wilson**, None; **S. Barnes**, None; **J.J. Nichols**, Paragon Vision Sciences (R), Coopervision (R), Alcon (R), Bruder (R), Johnson and Johnson Vision (R), Mallinckrodt (R)

### References

1. Aranha dos Santos V, Schmetterer L, Gröschl M, et al. In vivo tear film thickness measurement and tear film dynamics visualization using spectral domain optical coherence tomography. *Opt Express*. 2015;23(16):21043.
2. King-Smith PE, Fink BA, Fogt N, Nichols KK, Hill RM, Wilson GS. The thickness of the human precorneal tear film: evidence from reflection spectra. *Invest Ophthalmol Vis Sci*. 2000;41:3348–3359.
3. Werkmeister RM, Alex A, Kaya S, et al. Measurement of tear film thickness using ultrahigh-resolution optical coherence tomography. *Invest Ophthalmol Vis Sci*. 2013;54:5578–5583.
4. King-Smith PE, Nichols JJ, Nichols KK, Fink BA, Braun RJ. Contributions of evaporation and other mechanisms to tear film thinning and break-up. *Optom Vis Sci*. 2008;85:623–630.
5. Kimball SH, King-Smith PE, Nichols JJ. Evidence for the major contribution of evaporation to tear film thinning between blinks. *Invest Ophthalmol Vis Sci*. 2010;51:6294–6297.
6. Ewen King-Smith P, Reuter KS, Braun RJ, Nichols JJ, Nichols KK. Tear film breakup and structure studied by simultaneous video recording of fluorescence and tear film lipid layer images. *Invest Ophthalmol Vis Sci*. 2013;54:4900–4909.
7. Craig JP, Nelson JD, Azar DT, et al. TFOS DEWS II Report Executive Summary. *Ocular Surface*. 2017;15:802–812.
8. Liu H, Begley C, Chen M, et al. A link between tear instability and hyperosmolarity in dry eye. *Invest Ophthalmol Vis Sci*. 2009;50:3671–3679.
9. Braun RJ, King-Smith PE, Begley CG, Li L, Gewecke NR. Dynamics and function of the tear film in relation to the blink cycle. *Prog Retin Eye Res*. 2015;45:132–164.
10. Bron AJ, de Paiva CS, Chauhan SK, et al. TFOS DEWS II pathophysiology report. *Ocular Surface*. 2017;15:438–510.
11. Paulsen AJ, Cruickshanks KJ, Fischer ME, et al. Dry eye in the beaver dam offspring study: Prevalence, risk factors, and health-related quality of life. *Am J Ophthalmol*. 2014;157:799–806.
12. King-Smith PE, Hinel EA, Nichols JJ. Application of a novel interferometric method to investigate the relation between lipid layer thickness and tear film thinning. *Invest Ophthalmol Vis Sci*. 2010;51:2418–2423.
13. Bron AJ, Tiffany JM, Gouveia SM, Yokoi N, Voon LW. Functional aspects of the tear film lipid layer. *Exp Eye Res*. 2004;78:347–360.
14. Craig JP, Tomlinson A. Importance of the lipid layer in human tear film stability and evaporation. *Optom Vis Sci*. 1997;74:8–13.
15. Knop E, Knop N, Millar T, Obata H, Sullivan DA. The international workshop on meibomian gland dysfunction: report of the subcommittee on anatomy, physiology, and pathophysiology of the meibomian gland. *Invest Ophthalmol Vis Sci*. 2011;52:1938–1978.
16. Peng CC, Cerretani C, Li Y, et al. Flow evaporimeter to assess evaporative resistance of human tear-film lipid layer. *Ind Eng Chem Res*. 2014;53:18130–18139.

17. Bhamla MS, Chai C, Rabiah NI, Frostad JM, Fuller GG. Instability and breakup of model tear films. *Invest Ophthalmol Vis Sci.* 2016;57:949–958.
18. Georgiev GA, Eftimov P, Yokoi N. Structure-function relationship of tear film lipid layer: a contemporary perspective. *Exp Eye Res.* 2017;163:17–28.
19. Willcox MDP, Argüeso P, Georgiev GA, et al. TFOS DEWS II Tear Film Report. *Ocular Surface.* 2017;15:366–403.
20. Glasgow BJ. Evidence for phospholipids on the surface of human tears. *Invest Ophthalmol Vis Sci.* 2020;61(14):19.
21. Wizert A, Iskander DR, Cwiklik L. Organization of lipids in the tear film: a molecular-level view. *PLoS One.* 2014;9(3):e92461.
22. Butovich IA. Tear film lipids. *Exp Eye Res.* 2013;117:4–27.
23. Green-Church KB, Butovich I, Willcox M, et al. The international workshop on meibomian gland dysfunction: report of the subcommittee on tear film lipids and lipid-protein interactions in health and disease. *Invest Ophthalmol Vis Sci.* 2011;52:1979–1993.
24. Schaumberg DA, Nichols JJ, Papas EB, Tong L, Uchino M, Nichols KK. The international workshop on meibomian gland dysfunction: report of the subcommittee on the epidemiology of, and associated risk factors for, MGD. *Invest Ophthalmol Vis Sci.* 2011;52:1994–2005.
25. Daniel Nelson J, Shimazaki J, Benitez-del-Castillo JM, et al. The international workshop on meibomian gland dysfunction: report of the definition and classification subcommittee. *Invest Ophthalmol Vis Sci.* 2011;52:1930–1937.
26. Craig JP, Blades K, Patel S. Tear lipid layer structure and stability following expression of the meibomian glands. *Ophthalmic Physiol Opt.* 1995;15:569–574.
27. Arciniega JC, Wojtowicz JC, Mohamed EM, McCulley JP. Changes in the evaporation rate of tear film after digital expression of meibomian glands in patients with and without dry eye. *Cornea.* 2011;30:843–847.
28. Lemp MA, Crews LA, Bron AJ, Foulks GN, Sullivan BD. Distribution of aqueous-deficient and evaporative dry eye in a clinic-based patient cohort: a retrospective study. *Cornea.* 2012;31:472–478.
29. Lemp MA, Nichols KK. Blepharitis in the United States 2009: a survey-based perspective on prevalence and treatment. *Ocular Surface.* 2009;7(2 Suppl):S1–S14.
30. Tong L, Chaurasia SS, Mehta JS, Beuerman RW. Screening for meibomian gland disease: Its relation to dry eye subtypes and symptoms in a tertiary referral clinic in Singapore. *Invest Ophthalmol Vis Sci.* 2010;51:3449–3454.
31. Viso E, Gude F, Rodríguez-Ares MT. The association of meibomian gland dysfunction and other common ocular diseases with dry eye: a population-based study in Spain. *Cornea.* 2011;30:1–6.
32. Korb DR, Blackie CA. Meibomian gland diagnostic expressibility: correlation with dry eye symptoms and gland location. *Cornea.* 2008;27:1142–1147.
33. Lee Y, Hyon JY, Jeon HS. Characteristics of dry eye patients with thick tear film lipid layers evaluated by a LipiView II interferometer. *Graefes Arch Clin Exp Ophthalmol.* 2021;259:1235–1241.
34. Fenner BJ, Tong L. More to stable tears than thickness of the tear film lipid layer. *Invest Ophthalmol Vis Sci.* 2015;56:1601.
35. King-Smith PE, Braun RJ. Author response: More to stable tears than thickness of the lipid layer. *Invest Ophthalmol Vis Sci.* 2015;56:1602.
36. Butovich IA, Lu H, McMahan A, et al. Biophysical and morphological evaluation of human normal and dry eye meibum using hot stage polarized light microscopy. *Invest Ophthalmol Vis Sci.* 2013;55:87–101.
37. Rantamäki AH, Javanainen M, Vattulainen I, Holopainen JM. Do lipids retard the evaporation of the tear fluid? *Invest Ophthalmol Vis Sci.* 2012;53:6442–6447.
38. Rantamäki AH, Wiedmer SK, Holopainen JM. Melting points—the key to the anti-evaporative effect of the tear film wax esters. *Invest Ophthalmol Vis Sci.* 2013;54:5211–5217.
39. Sassa T, Tadaki M, Kiyonari H, Kihara A. Very long-chain tear film lipids produced by fatty acid elongase ELOVL1 prevent dry eye disease in mice. *FASEB J.* 2018;32:2966–2978.
40. Walter SD, Gronert K, McClellan AL, Levitt RC, Sarantopoulos KD, Galor A.  $\omega$ -3 tear film lipids correlate with clinical measures of dry eye. *Invest Ophthalmol Vis Sci.* 2016;57:2472–2478.
41. Bland HC, Moilanen JA, Ekholm FS, Paananen RO. Investigating the role of specific tear film lipids connected to dry eye syndrome: a study on O-Acyl- $\omega$ -hydroxy fatty acids and diesters. *Langmuir.* 2019;35:3545–3552.
42. Butovich IA, Wojtowicz JC, Molai M. Human tear film and meibum. Very long chain wax esters and (O-acyl)- $\omega$ -hydroxy fatty acids of meibum. *J Lipid Res.* 2009;50:2471–2485.
43. Miyamoto M, Sassa T, Sawai M, Kihara A, Radhakrishnan A. Lipid polarity gradient formed by  $\omega$ -hydroxy lipids in tear film prevents dry eye disease. *eLife.* 2020;9:e53582.
44. Paananen RO, Viitaja T, Olżyńska A, Ekholm FS, Moilanen J, Cwiklik L. Interactions of polar lipids with cholesteryl ester multilayers elucidate tear film lipid layer structure. *Ocular Surface.* 2020;18:545–553.
45. Schuett BS, Millar TJ. An investigation of the likely role of (O-acyl)  $\omega$ -hydroxy fatty acids in meibomian lipid films using (O-oleyl)  $\omega$ -hydroxy palmitic acid as a model. *Exp Eye Res.* 2013;115:57–64.
46. Brown SHJ, Kunnen CME, Duchoslav E, et al. A comparison of patient matched meibum and tear lipidomes. *Invest Ophthalmol Vis Sci.* 2013;54:7417–7423.
47. Butovich IA. On the presence of (O-acyl)- $\omega$ -hydroxy fatty acids and of their esters in human meibomian gland secretions. *Invest Ophthalmol Vis Sci.* 2011;52:639–641.
48. Chen J, Nichols KK. Comprehensive shotgun lipidomics of human meibomian gland secretions using MS/MS with successive switching between acquisition polarity modes. *J Lipid Res.* 2018;59:2223–2236.
49. Lam SM, Tong L, Yong SS, et al. Meibum lipid composition in Asians with dry eye disease. *PLoS One.* 2011;6(10):e24339.
50. Mori N, Fukano Y, Arita R, et al. Rapid identification of fatty acids and (O-acyl)- $\omega$ -hydroxy fatty acids in human meibum by liquid chromatography/high-resolution mass spectrometry. *J Chromatogr A.* 2014;1347:129–136.
51. Lam SM, Tong L, Duan X, et al. Longitudinal changes in tear fluid lipidome brought about by eyelid-warming treatment in a cohort of meibomian gland dysfunction. *J Lipid Res.* 2014;55:1959–1969.
52. Hancock SE, Ailuri R, Marshall DL, et al. Mass spectrometry-directed structure elucidation and total synthesis of ultra-long chain (O-acyl)- $\omega$ -hydroxy fatty acids. *J Lipid Res.* 2018;59:1510–1518.
53. Liebisch G, Vizcaíno JA, Köfeler H, et al. Shorthand notation for lipid structures derived from mass spectrometry. *J Lipid Res.* 2013;54:1523–1530.
54. Marshall DL, Saville JT, Maccarone AT, et al. Determination of ester position in isomeric (O-acyl)-hydroxy fatty acids by ion trap mass spectrometry. *Rapid Commun Mass Spectrom.* 2016;30:2351–2359.
55. Schiffman RM, Christianson MD, Jacobsen G, Hirsch JD, Reis BL. Reliability and validity of the ocular surface disease index. *Arch Ophthalmol.* 2000;118:615–621.
56. Bai Y, Ngo W, Khanal S, Nichols KK, Nichols JJ. Human precorneal tear film and lipid layer dynamics in

- meibomian gland dysfunction [published online ahead of print March 23, 2021]. *Ocular Surface*, <https://doi.org/10.1016/j.jtos.2021.03.006>.
57. Bron AJ, Benjamin L, Snibson GR. Meibomian gland disease. Classification and grading of lid changes. *Eye*. 1991;5:395–411.
  58. Tomlinson A, Bron AJ, Korb DR, et al. The international workshop on meibomian gland dysfunction: report of the diagnosis subcommittee. *Invest Ophthalmol Vis Sci*. 2011;52:2006–2049.
  59. Chen J, Green KB, Nichols KK. Quantitative profiling of major neutral lipid classes in human meibum by direct infusion electrospray ionization mass spectrometry. *Invest Ophthalmol Vis Sci*. 2013;54:5730–5753.
  60. Chen J, Green-Church KB, Nichols KK. Shotgun lipidomic analysis of human meibomian gland secretions with electrospray ionization tandem mass spectrometry. *Invest Ophthalmol Vis Sci*. 2010;51:6220–6231.
  61. Chen J, Nichols KK, Wilson L, Barnes S, Nichols JJ. Untargeted lipidomic analysis of human tears: a new approach for quantification of O-acyl-omega hydroxy fatty acids. *Ocular Surface*. 2019;17:347–355.
  62. Haworth KM, Nichols JJ, Thangavelu M, Sinnott LT, Nichols KK. Examination of human meibum collection and extraction techniques. *Optom Vis Sci*. 2011;88:525–533.
  63. Ngo W, Chen J, Panthi S, Nichols KK, Nichols JJ. Comparison of collection methods for the measure of human meibum and tear film-derived lipids using mass spectrometry. *Curr Eye Res*. 2018;43:1244–1252.
  64. Bai Y, Ngo W, Gu B, Zhang Y, Nichols JJ. An imaging system integrating optical coherence tomography and interferometry for in vivo measurement of the thickness and dynamics of the tear film. *Biomed Eng Online*. 2018;17(1):164.
  65. Team RC. *R: A Language and Environment for Statistical Computing*. 2020.
  66. Team RS. *RStudio: Integrated Development Environment for R*. 2020.
  67. Borchman D, Foulks GN, Yappert MC, Milliner SE. Changes in human meibum lipid composition with age using nuclear magnetic resonance spectroscopy. *Invest Ophthalmol Vis Sci*. 2012;53:475–482.
  68. Mudgil P, Borchman D, Yappert MC, et al. Lipid order, saturation and surface property relationships: a study of human meibum saturation. *Exp Eye Res*. 2013;116:79–85.
  69. King-Smith PE, Nichols JJ, Braun RJ, Nichols KK. High resolution microscopy of the lipid layer of the tear film. *Ocular Surface*. 2011;9:197–211.
  70. Cwiklik L. Tear film lipid layer: a molecular level view. *Biochim Biophys Acta*. 2016;1858:2421–2430.
  71. Nichols JJ, Mitchell GL, King-Smith PE. Thinning rate of the precorneal and prelens tear films. *Invest Ophthalmol Vis Sci*. 2005;46:2353–2361.
  72. Butovich IA. Meibomian glands, meibum, and meibogenesis. *Exp Eye Res*. 2017;163:2–16.
  73. King-Smith PE, Bailey MD, Braun RJ. Four characteristics and a model of an effective tear film lipid layer. *Ocular Surface*. 2013;11:236–245.
  74. King-Smith PE, Fink BA, Nichols JJ, Nichols KK, Braun RJ, McFadden GB. The contribution of lipid layer movement to tear film thinning and breakup. *Invest Ophthalmol Vis Sci*. 2009;50:2747–2756.
  75. Kulovesi P, Rantamaki AH, Holopainen JM. Surface properties of artificial tear film lipid layers: effects of wax esters. *Invest Ophthalmol Vis Sci*. 2014;55:4448–4454.
  76. Paananen RO, Javanainen M, Holopainen JM, Vattulainen I. Crystalline wax esters regulate the evaporation resistance of tear film lipid layers associated with dry eye syndrome. *J Phys Chem Lett*. 2019;10:3893–3998.